JOURNAL OF SPACECRAFT AND ROCKETS
Vol. 31, No. 2, March–April 1994

Monte Carlo Simulation of Launch Site Winds at Kennedy Space Center

Eric M. Queen*
NASA Langley Research Center, Hampton, Virginia 23681
Michael S. Warner†
George Washington University, Hampton, Virginia 23681
and
Daniel D. Moerder‡
NASA Langley Research Center, Hampton, Virginia 23681

This paper develops an easily implemented model for simulating random horizontal wind profiles over the Kennedy Space Center (KSC) at Cape Canaveral, Florida. The model is intended for use in Monte Carlo launch vehicle simulations of the type employed in mission planning. In this type of simulation, the large number of profiles needed for statistical fidelity of such simulation experiments makes the use of actual wind measurements impractical. The model is based on measurements made at KSC and represents vertical correlations by a decaying exponential model that is parameterized via least-squares parameter fit to the sample data. The model is demonstrated by comparing two open-loop Monte Carlo simulations of an asymmetric, heavy-lift launch vehicle. In the first simulation, measured wind profiles are used, whereas in the second, the wind profiles are generated using the stochastic model. The simulations indicate that the use of either the measured or simulated wind field results in similar launch vehicle performance. Although the model documented here is based on winter data, it can easily be adapted to other seasons.

I. Introduction

RANDOMLY varying launch site wind fields induce variations in sideforce and dynamic pressure on boosters during first-stage ascent flight. The fact that these load variations can affect the integrity of the vehicle structure and/or payload motivates interest in understanding and quantifying the effects of wind variations on the vehicle. The probabilistic distribution of these effects can be estimated by Monte Carlo simulation, but such simulation can require thousands of independent experiments to obtain "tight" estimates of the wind-induced loads. The expense of obtaining and archiving large numbers of measured wind profiles has motivated development of synthetic random wind simulation models. A number of studies conducted during the 1960s[1,2] resulted in simulation models in which wind variation was represented via analog transfer functions[1] and by multistep regression models.[2] More recently, modeling of wind profiles was treated as a demonstration of a low-order stochastic realization scheme.[3] This approach leads to multistep, autoregressive models whose covariance satisfies an error criterion established by the covariance of the actual measured data.

Another approach to the synthesis of wind profiles is used in the Global Random Atmosphere Model (GRAM).[4,5] GRAM is a worldwide database of point statistics for northerly and easterly (N/E) winds, in addition to atmospheric density, temperature, and pressure. Sample profiles are realized from the database via a simple first-order Markov perturbation model, under an assumption that the processes are Gaussian. The Markov model is formulated so that the pointwise means, variances, and correlations are reproduced exactly from the database. Correlations between parameters at different altitudes and locations are assumed to decay exponentially with distance.

In the next section of the paper, a collection of wind data from the Kennedy Space Center (KSC) launch site during the winter months is statistically characterized and used to develop a simple one-step wind simulation model in which northerly and easterly winds are assumed to be correlated Gaussian processes. The validity of this assumption is evaluated by statistical goodness-of-fit testing. The model represents ascending vertical correlations by a decaying exponential model that is parameterized via a least-squares fit to the sample data. Section III presents a comparative boost vehicle Monte Carlo simulation study. Two simulations of ascent flight for an asymmetric heavy-lift launch vehicle are compared. In the first simulation, the measured wind profiles are used, whereas in the second, the wind profiles are generated using the stochastic model. Appendix A describes a numerical experiment illustrating assumptions about the measured wind data. Appendix B describes of the process used to determine the coefficients of the model.

II. Model Development

This section describes development of the wind simulation model. The wind measurement data on which the model is based were provided to the authors courtesy of the Marshall Space Flight Center (MSFC). These data consist of horizontal wind velocities and azimuths, tabulated on altitude, for 450 "Jimsphere" profiles measured at KSC between 1964 and 1972. Jimspheres are aluminized spherical balloons that are released at ground level and tracked by FPS-16 radar as they ascend to measure winds aloft. This approach to measurement assumes that the balloon is entrained in the air mass and that the air mass velocity is uniform at each altitude along the groundtrack flown by the balloon. All of the Jimsphere profiles used were taken during the months of December through February. These months were selected for study because the

Received Aug. 8, 1992; revision received Nov. 10, 1992; accepted for publication Nov. 21, 1992.

*Aerospace Technologist, Spacecraft Control Branch. Member AIAA.
†Graduate Student, Joint Institute for Advancement of Flight Sciences, NASA Langley Research Center. Student Member AIAA.
‡Senior Research Engineer, Spacecraft Control Branch. Senior Member AIAA.

winter wind environment at KSC is the most difficult for launch operations. The winter winds have larger means and larger variations about those means.

For each month of data, 150 profiles were supplied, with data represented at vertical intervals of 25 m from ground level up to 20 km. These data are measured in velocity/azimuth format by radar at KSC at altitude intervals between 25 and 150 m, depending on altitude and conditions. The profiles are then smoothed by a combination of automated and manual means before being stored at 25-m increments and delivered to MSFC. A number of the profiles were missing data either near the ground or near the top of the profile. Figure 1 displays the number of samples available in the winter data set as a function of altitude.

Verification of the assumption that the wind data are jointly Gaussian at each altitude was done via goodness-of-fit testing.[6] Statistical goodness-of-fit testing is done by constructing a measure of the error between the sample statistics of a given population of data and those of the model distribution. This measure, itself a random variable, is chosen in such a manner that its probability distribution is known. The "significance" of the goodness-of-fit is used to determine the appropriateness of using a given model for a given distribution. The significance is defined as the probability that, given the assumption that the sample population did indeed come from the model distribution, a larger error could have been observed. In other words, it is the probability that the test user would be wrong if he or she concluded that the sample population was not drawn from the model distribution. For further details on statistical goodness-of-fit testing, the reader is referred to Ref. 6.

The assumption that the N/E wind data are jointly Gaussian was tested via two-dimensional chi-squared tests at each altitude, with significance results shown in the top of Fig. 2. The chi-squared test is based on frequencies in binned data. Bins were chosen for joint N/E velocity intervals such that each bin at each altitude contained at least five elements. The variation in the number of bins with altitude is illustrated by the plot at the bottom of Fig. 2, which displays the number of degrees of freedom (n_χ) for the chi-squared random variables at each altitude, given by

$$n_\chi = n_{\text{bins}} - n_{\text{constraints}} - 1$$

where the first two statistical moments in the bivariate distribution provided five constraints.

Examination of the significance plot indicates that this was a rather noisy test, and that the average value of the fit

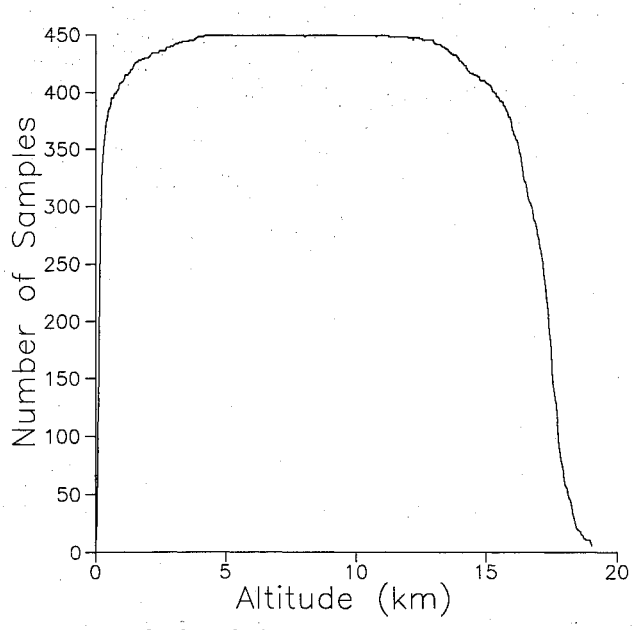

Fig. 1 Number of wind data samples at each altitude.

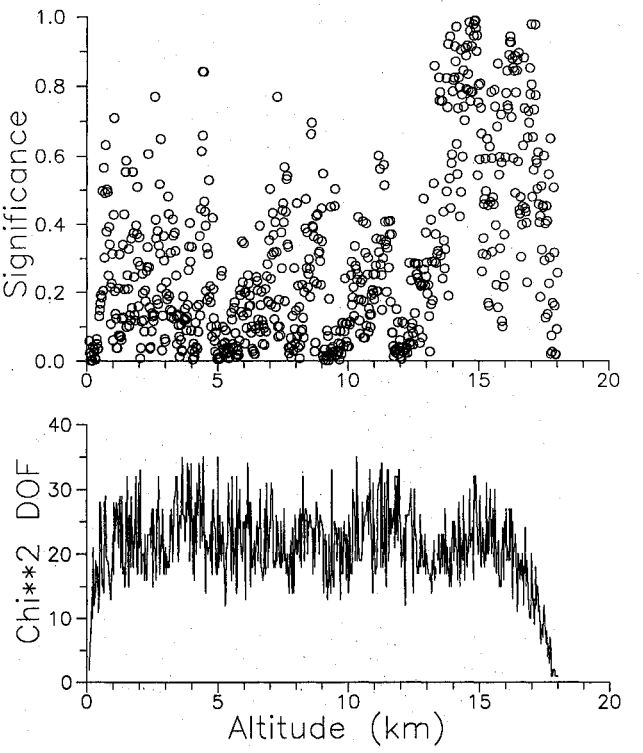

Fig. 2 Results of two-dimensional chi-squared tests on the north/east wind data.

significance was approximately 35%. According to standard interpretations of these tests,[6] this indicates an adequate fit to a bivariate Gaussian distribution at most altitudes. Higher significance values would, however, provide stronger confidence in the model. One possible explanation for the observed spread in significance values stems from processing that the wind data underwent before they became available to the authors. It is possible that this processing introduced effects into the data that, upon performing the nonlinear transformation from velocity/azimuth (V/A) into N/E coordinates, resulted in the small non-Gaussian distortions seen in Fig. 2. Figure 3 displays significances for the separate fits of the N/E winds to their assumed marginal Gaussian distributions. These significances were obtained using the Kolmogorov-Smirnov (KS) test,[6] which is applicable to continuous univariate random variables. It can be seen that these marginal fits (Fig. 3) are significantly better than the joint fit (Fig. 2), which is consistent with the hypothesis that the distortion stems from data processing in V/A coordinates. Appendix A presents a numerical experiment that suggests that the Gaussian nature of the distributed data could have been degraded by smoothing of the raw Jimsphere tracking data. Given the potential for uncertainty due to data smoothing and the relatively small sample size (≤ 450 samples), the results displayed in Figs. 2 and 3 suggest that the Gaussian model is an adequate representation of the wind process.

Having verified that the available data for KSC launch site winds are adequately described by a probabilistic model that is Gaussian at each altitude, a Gaussian simulation model is developed based on the observed sample statistics. The N/E simulated winds $\hat{W}(h)$ are given by

$$\hat{W}_K(h) = m_K(h) + \delta_K(h) \qquad K = N, E \tag{1}$$

where the sample means $m_K(h)$ estimate the population means

$$\mu_K(h) = \mathcal{E}[W_K(h)] \qquad K = N, E \tag{2}$$

where $W_K(h)$ is the K-component of measured wind at altitude h, $\mathcal{E}$ is the expectation operator, and $\delta_K(h)$ are mutually

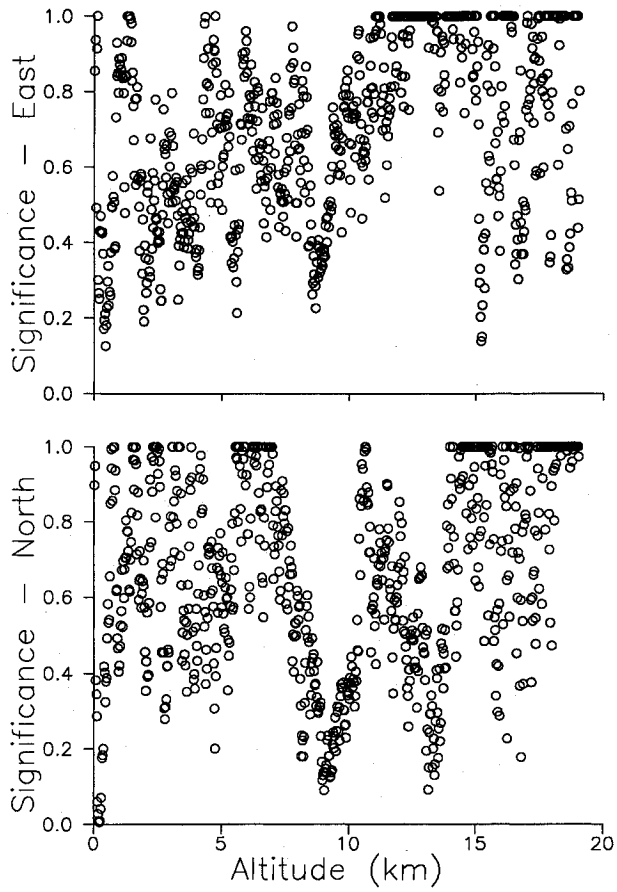

Fig. 3 Komolgorov-Smirnov statistic with altitude for east and north winds.

correlated random perturbation terms given by

$$\begin{bmatrix}\delta_E(h)\\ \delta_N(h)\end{bmatrix} = \begin{bmatrix}s_E(h) & 0\\ r_\nu(h)s_N(h) & s_N(h)\sqrt{1-r_\nu^2(h)}\end{bmatrix}\begin{bmatrix}\nu_E(h)\\ \nu_N(h)\end{bmatrix} \quad (3)$$

where the sample variances $s_K^2(h)$ estimate the population variances

$$\sigma_K^2(h) = \mathcal{E}\{[W_K(h) - \mu_K(h)]^2\} \quad (4)$$

The sample correlation coefficient $r_\nu(h)$ is an estimate of

$$\rho_{NE}(h) = \frac{\mathcal{E}\{[W_E(h) - \mu_E(h)][W_N(h) - \mu_N(h)]\}}{\sigma_N(h)\sigma_E(h)} \quad (5)$$

and the ν_K are independent first-order Gauss-Markov processes. The sample means and standard deviations in Eqs. (1) and (3) are displayed in Figs. 4 and 5 and r_{NE} is displayed in Fig. 6. The ν_K are propagated as

$$\nu_K(h) = \tilde{a}_K(h, h - \Delta h)\cdot \nu_K(\mathrm{h} - \Delta h) + \sqrt{1 - \tilde{a}_K^2(h, h - \Delta h)}\cdot g_K(h) \quad (6)$$

where $g_K(h)$ are independent standard normal random numbers. The parameters $a_K(h, \Delta h)$ are functions chosen such that the vertical correlations of the $\delta_K(h)$ approximately satisfy the observed sample vertical correlation coefficients, $r_K(h, h - \Delta h)$, which in turn estimate

$$\rho_K(h, h - \Delta h) = \frac{\mathcal{E}\{[W_K(h) - \mu_K(h)][W_k(h - \Delta h) - \mu_K(h - \Delta h)]\}}{\sigma_K(h)\sigma_K(h - \Delta h)} \quad (7)$$

for $K = N,E$.

Two functional forms for $a_K(h, \Delta h)$, approximating $r_K(h, h - \Delta h)$, were considered. The first was exponential

$$a_K(h, \Delta h) = \exp[-\Delta h/b_K(h)] \qquad K = N, E \quad (8)$$

and the other was a combination of exponential with a constant offset:

$$a_K(h, \Delta h) = [1 - c_K(h)]\exp[-\Delta h/b_{1_K}(h)] + c_K(h) \quad (9)$$

where $0 \le c_K(h) \le 1$. The parameter vectors $b_K(h)$ and $b_{1_K}(h)$ were chosen by a least-squares fit to the $r_K(h, h - \Delta h)$ averaged over 200-m bins over a Δh range of 0–2.5 km. This 2.5-km "window" was chosen to provide a compromise between applicability of the model for large values of Δh and applicability of the model throughout the maximum number of altitudes available in the data. Details of the model selection and calculations are provided in Appendix B.

The $\tilde{a}_K(h, \Delta h)$ in Eq. (6) are related to the $a_K(h, \Delta h)$ in Eqs. (8) and (9) by

$$\tilde{a}_E(h, \Delta h) = a_E(h, \Delta h) \quad (10)$$

$$\tilde{a}_N(h, \Delta h) = \frac{a_N(h, \Delta h) - r_{NE}(h)r_{NE}(h - \Delta h)a_E(h, \Delta h)}{\sqrt{1 - r_{NE}^2(h)}\sqrt{1 - r_{NE}^2(h - \Delta h)}} \quad (11)$$

The expression Eq. (11) corrects the ν_N vertical correlation so that the correlation coefficient for δa_N approximates $r_N(h, h - \Delta h)$. This correction is necessitated by the fact that the δ_N are linear combinations of ν_E and ν_N.

The goodness-of-fit of the vertical correlation model to the actual data was evaluated by examining the error between the model and data as a function of h and Δh. This error is the difference $a_K(h, \Delta h) - r_K(h, h - \Delta h)$. The error surfaces for the simple exponential model for east and north winds are shown in Fig. 7. The error surfaces for the second model are shown in Fig. 8. Comparing the relative areas of large error, it is seen that the exponential-with-offset model gives a slightly

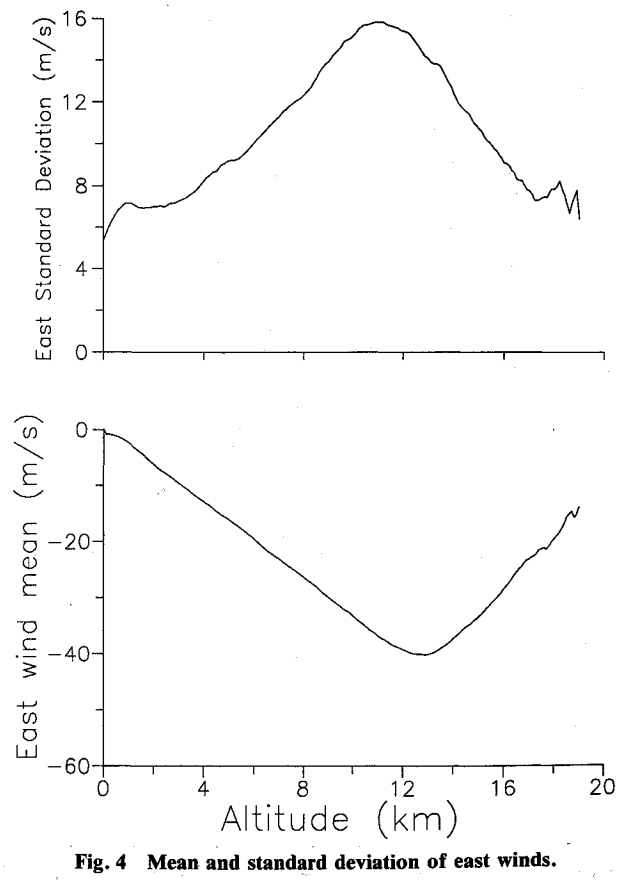

Fig. 4 Mean and standard deviation of east winds.

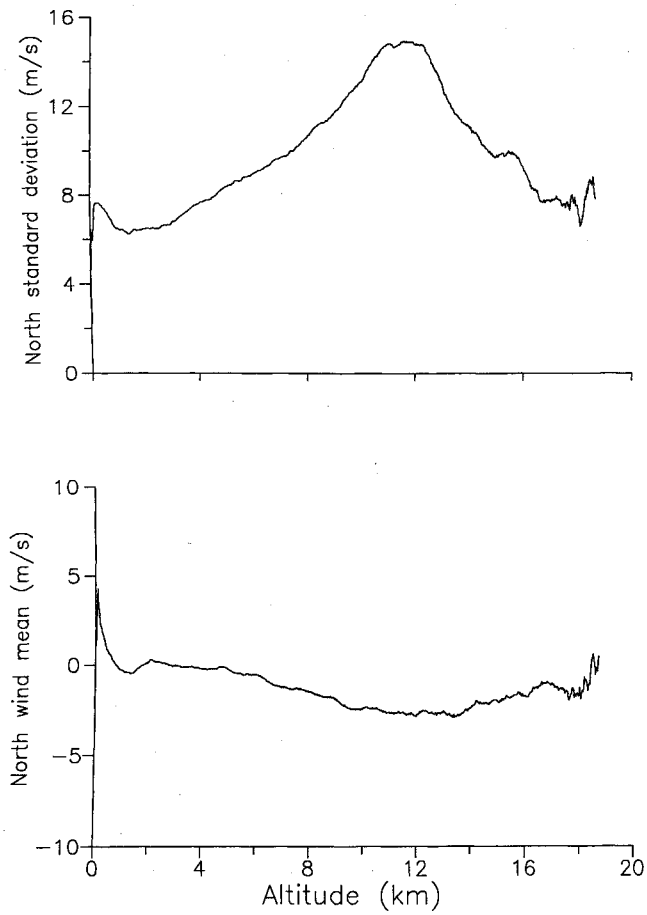

Fig. 5 Mean and standard deviation of north winds.

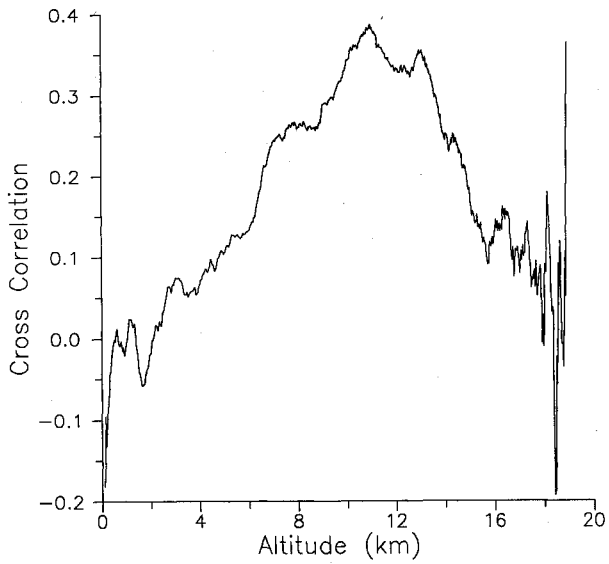

Fig. 6 Cross correlation between east and north winds with altitude.

better fit, especially at low altitudes. Based on these differences, the constant-offset model was chosen as the standard model.

III. Model Application

In this section, the wind model is demonstrated in a pair of Monte Carlo simulations that compare booster ascent trajectories subject to winds from the measured wind set against trajectories subject to synthetic winds from the simulation model.

The vehicle model is an asymmetric, single-booster configuration[7] from the Advanced Launch System (ALS) program. The three-degree-of-freedom simulation of this model uses winds input as tabular functions of altitude. All simulations were ascent trajectories run to 16.5-km altitude, since that is the highest altitude for which sufficient wind measurements were available. Staging was not an issue since it occurs at 153 s and the end condition (16.5-km altitude) was usually reached after about 77 s. The vehicle was controlled with an open-loop pitch-rate history, which was precalculated without considering winds.

In the validation of a statistical wind model for launch simulations, the values of maximum dynamic pressure q_{max}, the maximum product of dynamic pressure and angle of attack $|q\alpha|_{max}$, and the maximum product of dynamic pressure and sideslip angle $|q\beta|_{max}$ are important measures of the behavior of the simulation. These quantities are directly related to the aerodynamic loads experienced by the vehicle, and they are largely determined by the winds encountered. Other quantities of interest were $\int(q\alpha)^2\,dt$ and $\int(q\beta)^2\,dt$. Persistent differences between the magnitudes of the measured and simulated wind fields would manifest themselves in the relative values of these quantities.

The first Monte Carlo simulation consisted of 450 trajectories that incorporated the measured wind profile. Another 450 trajectories were simulated using wind profiles generated by the wind model with a vertical step of 200 m. From each of these 900 trajectories, the values of q_{max}, $|q\alpha|_{max}$, and $|q\beta|_{max}$ the times at which they occurred; and $\int(q\alpha)^2\,dt$ and $\int(q\beta)^2\,dt$ were recorded.

The sample means and standard deviations of these quantities, along with the 95% confidence intervals, based on 450 samples, are presented in Figs. 9 and 10, respectively. Note

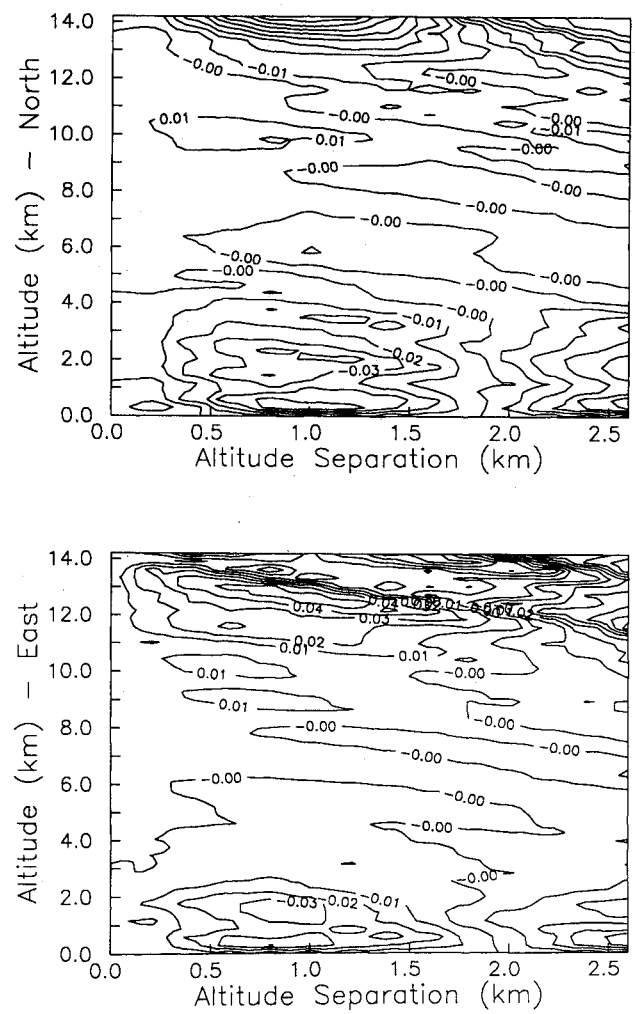

Fig. 7 First correlation coefficient model errors for east and north winds.

that, for these trajectories, the means and standard deviations of $|q\alpha|$ and $|q\beta|$-related quantities are of the same order of magnitude. The 95% confidence error bars overlap from the measured and simulated wind cases in most of the "max" and integral quantities, with the exceptions of the mean $|q\alpha|_{max}$ and the standard deviation of $|q\beta|_{max}$. Even though these tests indicate statistically significant differences in these particular quantities, the actual magnitudes of the differences are only on the order of 100 lbf · deg in each case. Furthermore, it should be noted that the assignment of 95% confidence levels here is based on an assumption of sampling from a Gaussian population, whereas $|q\alpha|_{max}$ and $|q\beta|_{max}$ are doubtless highly non-Gaussian.

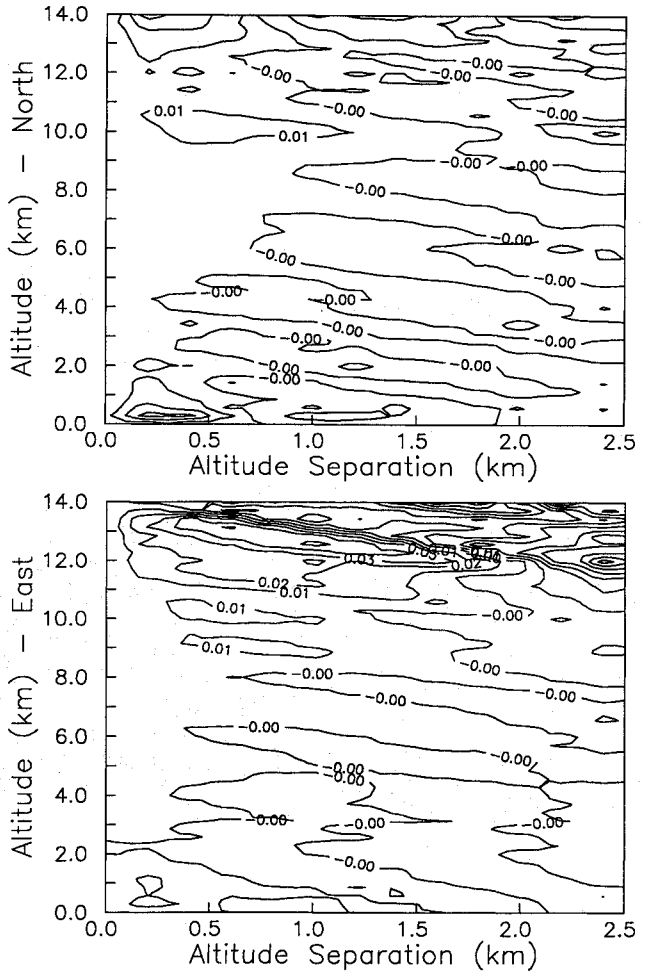

Fig. 8 Second correlation coefficient model errors for east and north winds.

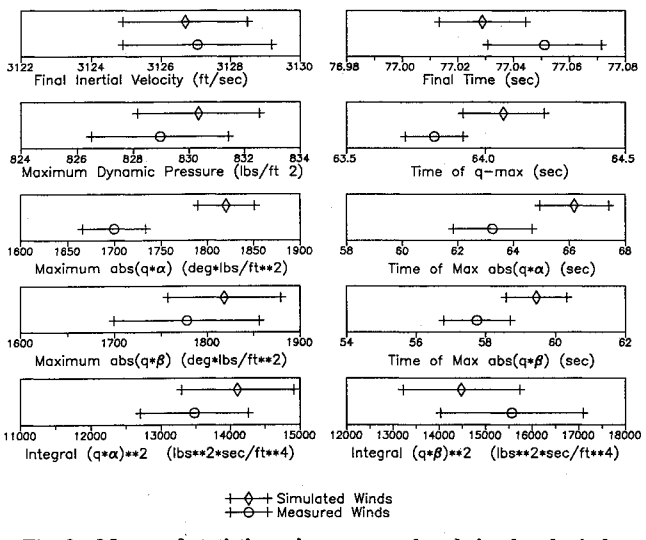

Fig. 9 Means of statistics using measured and simulated winds.

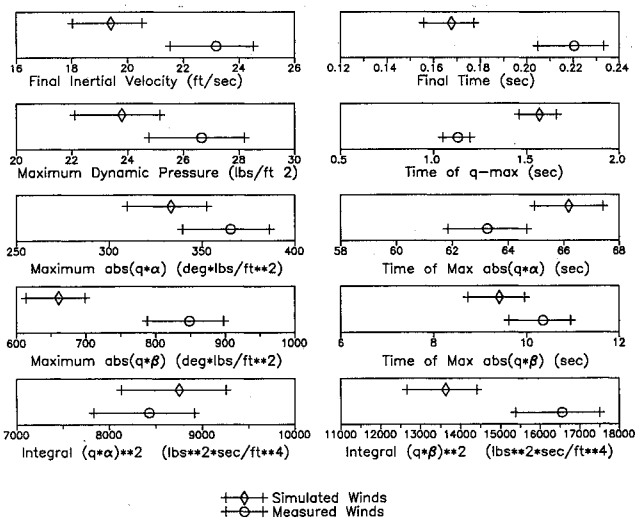

Fig. 10 Standard deviations of statistics using measured and simulated winds.

IV. Concluding Remarks

A KSC-specific launch site wind model has been developed and tested. This model is based on wind measurements made at KSC in the winter months over a period of several years. These measurements were statistically characterized, and the assumption that, at each altitude, they are distributed as bivariate Gaussian random variables in the northerly and easterly directions was examined. The wind model is propagated in altitude via a correlated pair of simple Markov processes. Subject to an assumption that wind process is Gaussian, the proposed model is a statistically accurate representation of launch site winds.

This model was demonstrated by comparing the results of two Monte Carlo simulations, one using simulated winds and the other using measured winds. The results of these simulations were within 95% confidence intervals for many important quantities of interest for simulations. Apparently significant deviations between simulation results for measured and synthetic winds suggest that more study of the modeling assumptions and execution is warranted.

Appendix A: Potential Impact of Data Smoothing

This Appendix supports the assertion that smoothing of the speed/azimuth data could have reduced the jointly Gaussian quality of the N/E wind data with little or no impact on its marginal distributions. First, 512 populations of normally distributed, bivariate pairs were generated. Each population consisted of 450 ordered samples. The number of samples corresponds to the maximum number of samples available at each altitude in the measured wind data. For clarity, the two members of each pair from population i, sample j, will be referred to as x_{ij}, y_{ij}. Note that with this ordering the populations can also be considered as 450 sequences of jointly Gaussian pairs with 512 members in each sequence. The pairs were generated with

$$E[x_{ij}] = E[y_{ij}] = 0$$

$$(\sigma_x)_{ij} = (\sigma_y)_{ij} = 1$$

where $E[x]$ denotes the expected value or mean of random process x, σ_x denotes the standard deviation of x, and

$$1 \le i \le 450$$

$$1 \le j \le 512$$

The cross correlation R_{xy} is given by

$$R_{x_{kl}y_{mn}} = 0.1$$

if $k = m$ and $l = n$ and, otherwise,

$$R_{x_{kl}y_{mn}} = 0$$

The populations were tested for goodness of fit to marginal and bivariate Gaussian distributions with the results illustrated in Figs. A1 and A2. Since these populations were explicitly

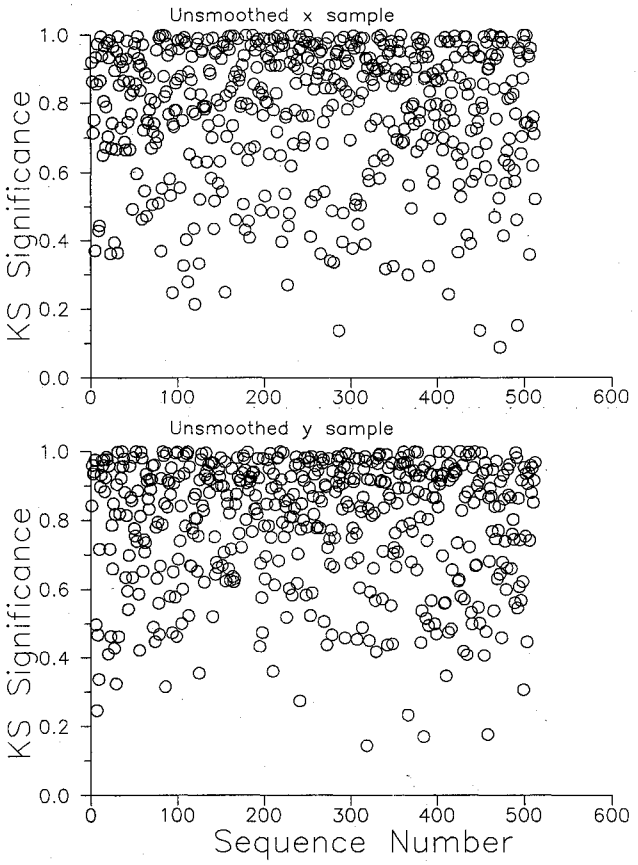

Fig. A1 Significance of Komolgorov-Smirnov statistic for unsmoothed x and y samples.

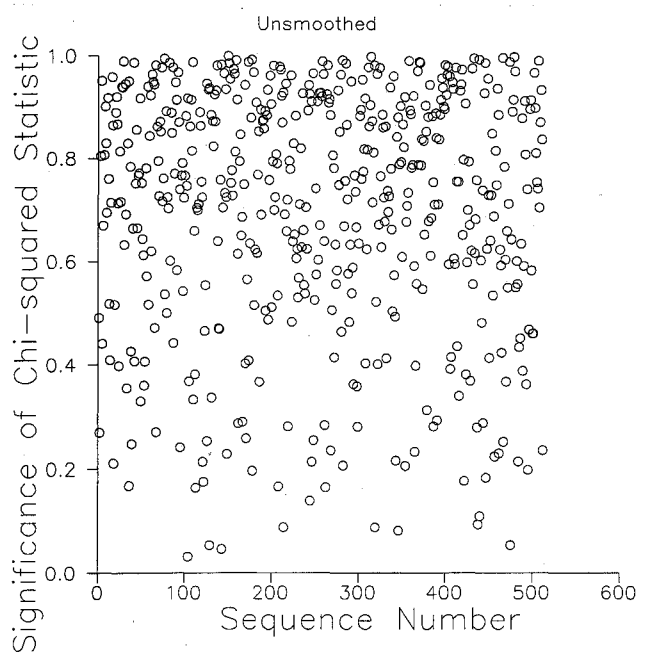

Fig. A2 Significance of joint chi-squared statistics for unsmoothed x and y samples.

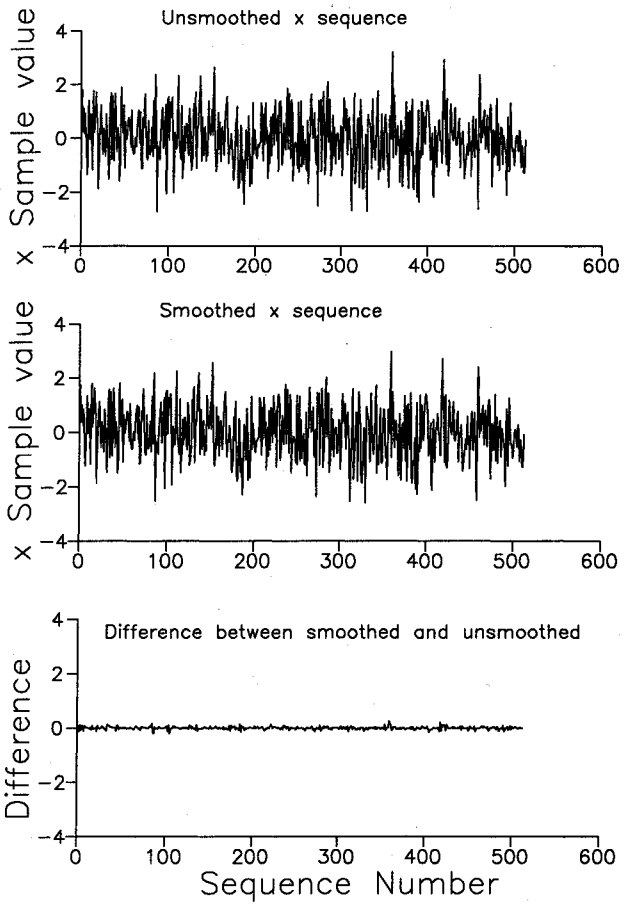

Fig. A3 Difference between sample smoothed and unsmoothed sequences.

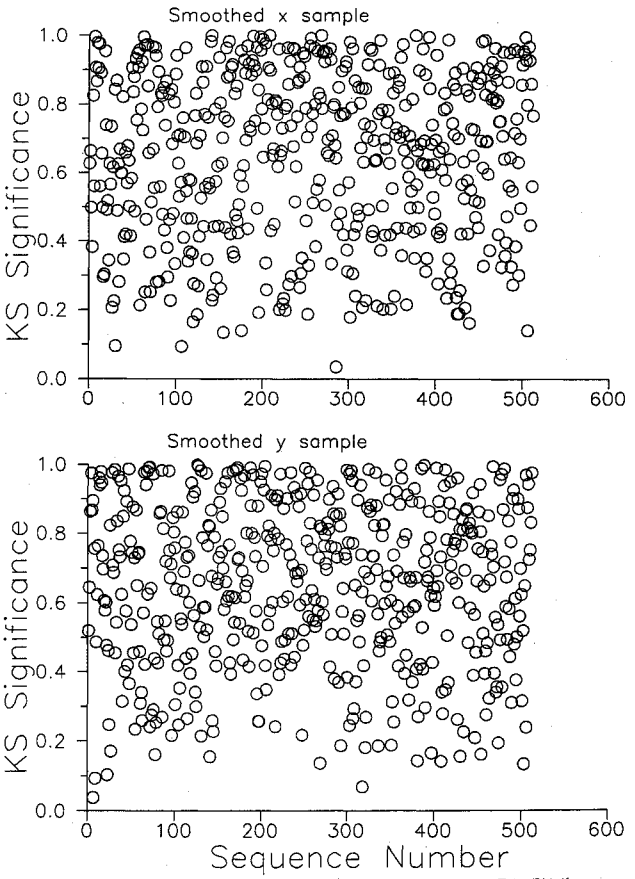

Fig. A4 Significance of Komolgorov-Smirnov statistic for smoothed x and y samples.

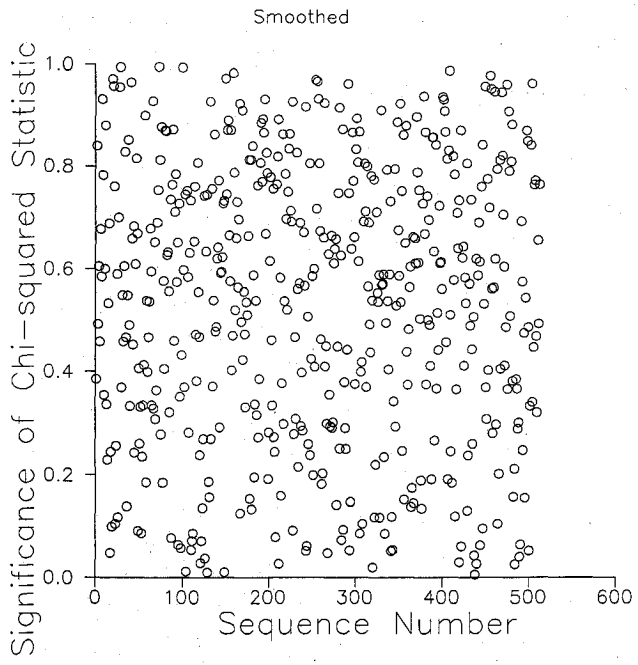

Fig. A5 Significance of joint chi-squared statistic for smoothed x and y samples.

generated as samples from the assumed distribution, they show the best goodness-of-fit probabilities that can be expected from these tests.

The population samples were next transformed by the relations

$$v_{i,j} = \sqrt{x_{ij}^2 + y_{ij}^2}$$

$$z_{i,j} = \tan^{-1}(y_{ij}/x_{ij})$$

This transformation is identical to that of changing winds from Cartesian to polar coordinates. The v_{ij} were then smoothed using a fast Fourier transform and a low-pass filter. This was done using the algorithm by Press et al.[8] with a window width of 1 point. Figure A3 shows a sample x_{ij} sequence before and after smoothing. The degree of smoothing is seen to be quite mild. The smoothed sequences were then converted back to Cartesian coordinates and the statistical tests were repeated. The results of these tests are shown in Figs. A4 and A5. Figure A4 shows the significance of the KS statistic for the marginal distributions as a function of sequence number. As with Fig. A3, there was good agreement with the assumed model. This degree of smoothing has little effect on the marginal statistics of the samples. Figure A5 shows the results of the chi-squared test of the bivariate Gaussian quality of the data. This figure indicates that the smoothed sequences are significantly less jointly Gaussian than the same data before smoothing.

Appendix B: Vertical Correlation Coefficient Model

This Appendix describes the process of determining the vertical autocorrelation coefficients for the simulated northerly and easterly winds as introduced in Sec. II.

Two structures for the autocorrelation coefficient model were investigated. In the first, the autocorrelation coefficient $r(h, \Delta h)$ is modeled as $\hat{r}(h, \Delta h)$, a decaying exponential with a scale distance b, defined as a function of altitude:

$$\hat{r}(h, \Delta h) = \exp[-\Delta h/b(h)] \tag{B1}$$

where Δh is the altitude increment between measured wind data points.

A second model was investigated that introduced a second scale distance $b_2(h)$ and a mixing factor c(h):

$$\hat{r}(h, \Delta h) = [1 - c(h)]\exp[-\Delta h/b_1(h)] + c(h)\exp[-\Delta h/b_2(h)] \tag{B2}$$

The additional parameters of the latter model were introduced to provide additional flexibility in achieving a close fit to the sample autocorrelation coefficients.

Values for the parameters for the two model structures were calculated at each altitude by minimizing $J(h)$, the squared deviation of the sample, and modeled autocorrelation coefficients:

$$J(h) = \sum_{i=1}^{k} [r(h, \tau_i) - \hat{r}(h, \tau_i)]^2$$

$$\tau_i = i\Delta h, \ \tau_{\max} = k\Delta h \tag{B3}$$

The deviations are summed over a range of altitude separations τ such that

$$0 < \tau < 2.5 \text{ km} \tag{B4}$$

as mentioned in Sec. II. The sample autocorrelation coefficient r is calculated as

$$r(h, \tau) = \frac{1}{s(h)s(h+\tau)} \frac{1}{N-1} \sum_{j=1}^{N} [w_j(h)w_j(h+\tau) - N\bar{w}(h)\bar{w}(h+\tau)] \tag{B5}$$

$$\bar{w}(h) = \frac{1}{N} \sum_{j=1}^{N} w_j(h) \tag{B6}$$

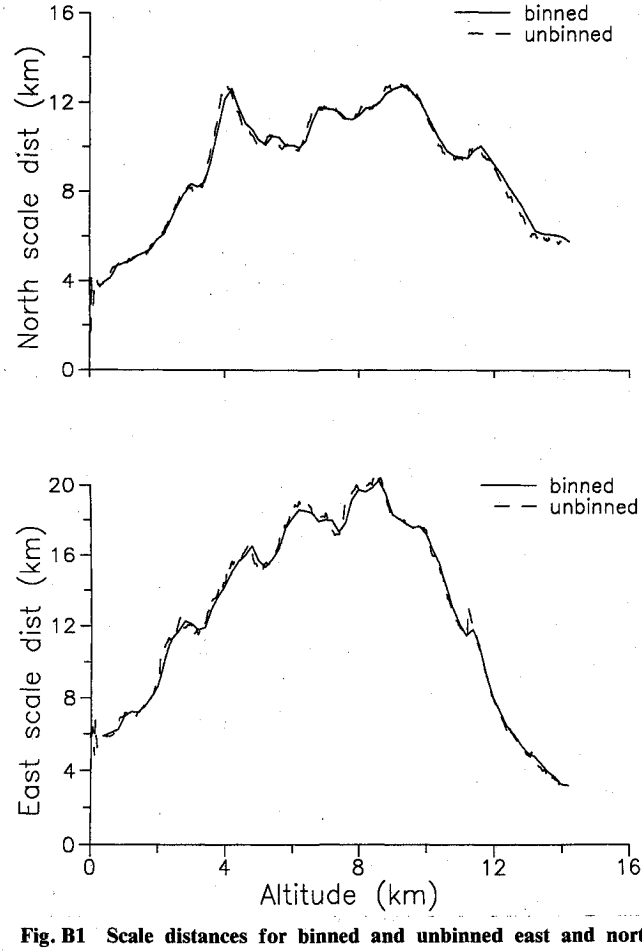

Fig. B1 Scale distances for binned and unbinned east and north winds (first correlation coefficient model).

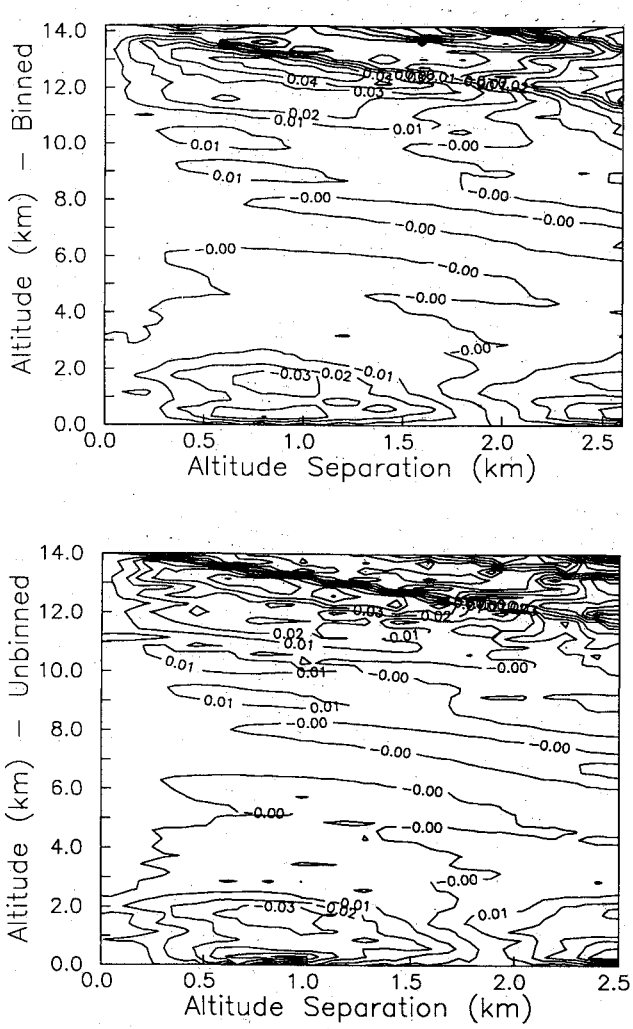

Fig. B2a Model errors for binned and unbinned east winds (first correlation coefficient model).

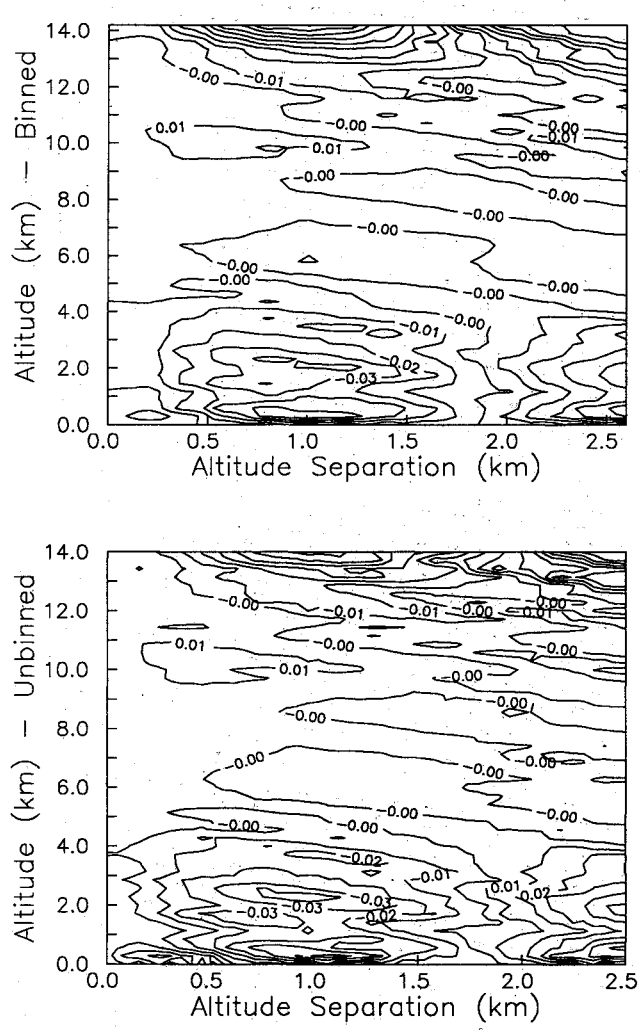

Fig. B2b Model errors for binned and unbinned north winds (first correlation coefficient model).

$$s^2(h) = \frac{1}{N-1}\sum_{j=1}^{N}[w_j^2(h) - N\bar{w}(h)] \tag{B7}$$

where w_j is the east or north component of the measured wind in the jth data profile, and N is the total number of profiles.

For each model, optimal model parameters were found using a quasi-Newton algorithm, with convergence criterion

$$\frac{\| \nabla J \|}{J} \leq 10^{-4} \tag{B8}$$

where ∇J represents the gradient of J with respect to the free parameters.

In running the optimization algorithm using the second model given by Eq. (B2), the autocorrelations at first violated the constraint that the autocorrelation be between zero and one. The problem was resolved by bounding the values of the mixing factor c and the second scale distance as follows:

$$0 < c < 1 \tag{B9}$$

$$b_1 < b_2 < 10{,}000 b_1 \tag{B10}$$

These inequality constraints were each implemented in the unconstrained minimization through use of Valentine transformations. These transformations yielded the following equality constraints in terms of two unconstrained model parameters, α_1 and α_2:

$$c = \sin^2(\alpha_1) \tag{B11}$$

$$b_2 = [1 + 100 \sin^2(\alpha_2)]^2 b_1 \tag{B12}$$

Using the modified optimization algorithm, approximate autocorrelation functions were calculated using model structures from Eqs. (B1) and (B2) at base altitudes up to 14 km. This altitude limit insured that a sufficient number of reasonable wind data pairs were available for calculating autocorrelation coefficients in Eq. (B3). Recall that the autocorrelations are modeled over an altitude separation of 2.5 km. Thus, from the highest base altitude, autocorrelations can be calculated up to 16.5 km, the highest altitude used in the ALS simulations discussed in Sec. III.

The resulting model parameters are in the form of tabular functions at the 560 altitude points (up to 14 km in 25-m increments). The effect of binning on the fidelity of the model was investigated in an effort to reduce this number. The original wind data were binned into 200-m altitude increments, and corresponding autocorrelations and model parameters were calculated. The results comparing the binned and unbinned cases are discussed next.

The scale distances for the first model over the altitude range are given in Fig. B1, and the corresponding error surfaces are presented in Fig. B2. Note that binning the wind data reduces the high-frequency content of the scale distance results, whereas the errors for the two cases are virtually identical.

For the second model, the optimal model parameters are given in Fig. B3. At the middle and highest altitudes for the north winds, the decrease in the scale distances in the binned case is compensated for by a corresponding increase in mixing

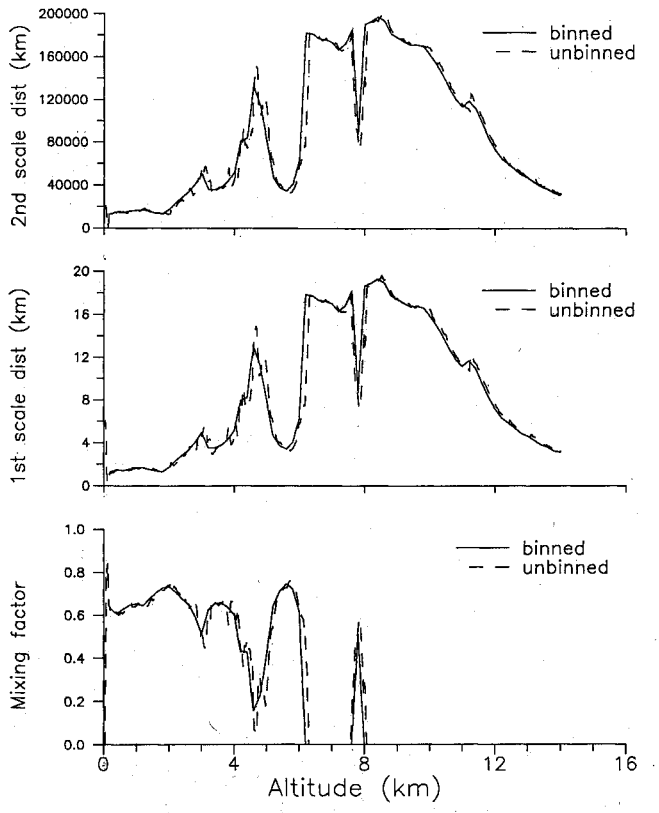

Fig. B3a Model parameters for binned and unbinned east winds (second correlation coefficient model).

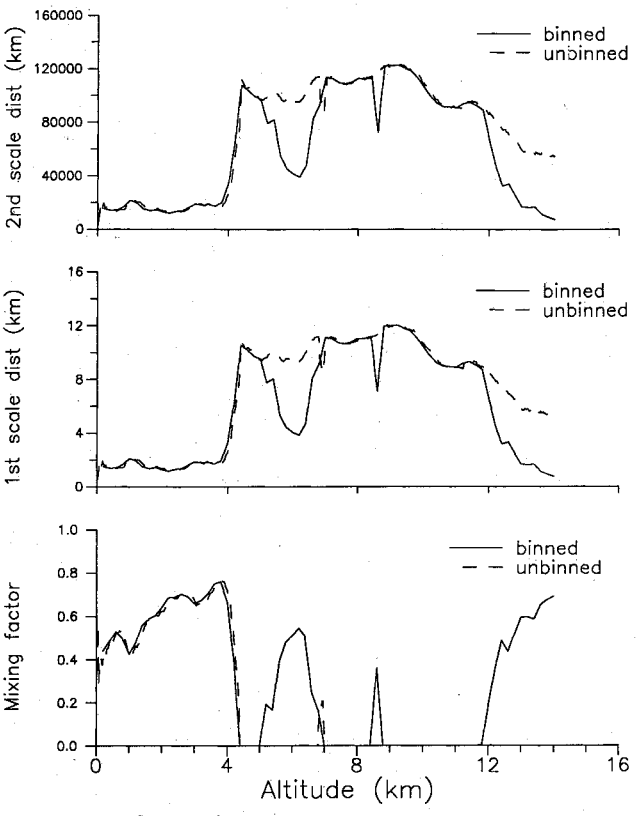

Fig. B3b Model parameters for binned and unbinned north winds (second correlation coefficient model).

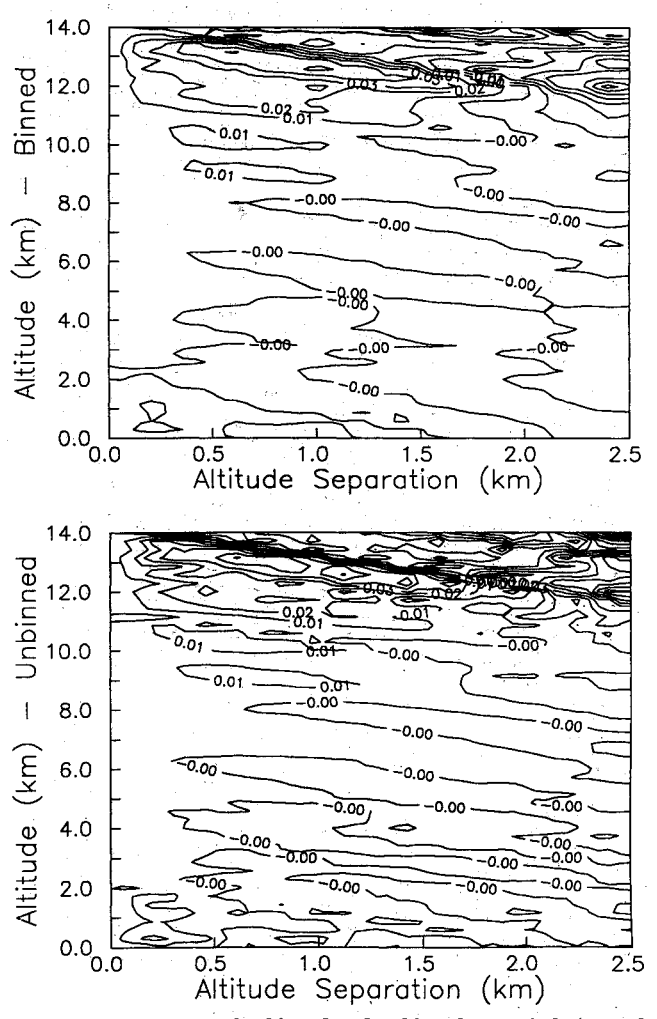

Fig. B4a Model errors for binned and unbinned east winds (second correlation coefficient model).

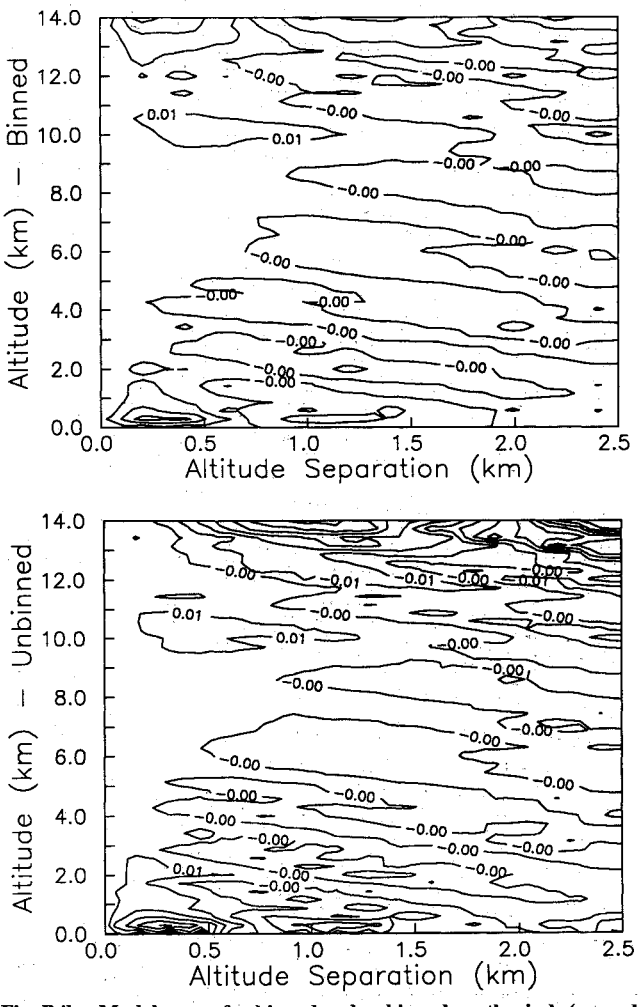

Fig. B4b Model errors for binned and unbinned north winds (second correlation coefficient model).

factor. Otherwise the results are virtually identical. The similarities in the error surfaces presented in Fig. B4 confirm the equivalence of the two sets of results.

Therefore, when the autocorrelation function is based on binned as opposed to unbinned wind data, it has only one-eighth the number of model parameters with an insignificant loss of accuracy. For this reason, binned results are used for further analysis in Sec. II.

Similarly, note that, in using either the binned or unbinned wind data, the second scale distance in general rode the maximizing constraint, effectively making the second term in Eq. (B2) a constant equal to the mixing factor. For this reason, the model was simplified by neglecting the second exponential function, leaving the model form as

$$\hat{r}(h, \Delta h) = [(1 - c(h)]\exp[-\Delta h / b_1(h)] + c(h) \qquad \text{(B13)}$$

This model form was used for the Monte Carlo simulations, as described in Sec. III.

References

[1]Gott, E., "Linear Regression of Interlevel Wind Velocities," *IEEE Transactions on Geoscience Electronics,* Vol. GE-7, No. 1, 1969, pp. 44–47.

[2]Bailey, J., Palmer, J., and Wheeler, R., "Launch Vehicle and Turbulence Response by Nonstationary Statistical Methods," NASA CR-846, Aug. 1967.

[3]Menga, G., and Sundarajan, N., "Stochastic Modeling of Mean-Wind Profiles for In-Flight Wind Estimation—A New Approach to Lower Order Stochastic Realization Schemes," *IEEE Transactions on Automatic Control,* Vol. AC-27, No. 3, 1982, pp. 547–558.

[4]Justus, C., Roper, R., Woodrum, A., and Smith, O., "Global Reference Atmosphere Model for Aerospace Applications," *Journal of Spacecraft and Rockets,* Vol. 12, No. 4, 1975, pp. 449,450.

[5]Justus, C., Fletcher, G., Gramling, F., and Pace, W., "The NASA/MSFC Global Reference Atmospheric Model—MOD 3 (with Spherical Harmonic Wind Model)," NASA CR-3256, March 1980.

[6]Guttman, I., Wilks, S., and Hunter, J., *Introductory Engineering Statistics,* Wiley, New York, 1971.

[7]Pamadi, B. N., and Dutton, K. E., "An Aerodynamic Model for ALS Vehicle," NASA TM, 1990 (to be published).

[8]Press, W. H., Flannery, B. P., Teukolsky, S. A., and Vetterling, W. T., *Numerical Recipes,* Cambridge Univ. Press, New York, 1986.

James A. Martin
Associate Editor